Naval Research Laboratory
Stennis Space Center, MS 39529-5004

NRL/FR/7322--96-9656

Tidal Elevations in the Yellow and East China Seas From a Data-Assimilative, Barotropic Tidal Model

CHERYL ANN BLAIN

Ocean Dynamics and Prediction Branch
Oceanography Division

July 3, 1997

REPORT DOCUMENTATION PAGE

Form Approved
OBM No. 0704-0188

1. AGENCY USE ONLY *(Leave blank)*	2. REPORT DATE	3. REPORT TYPE AND DATES COVERED
	July 3, 1997	Final

4. TITLE AND SUBTITLE

Tidal Elevations in the Yellow and East China Seas From a Data-Assimilative, Barotropic Tidal Model

5. FUNDING NUMBERS

Job Order No. 573509706
Program Element No. 0603207N
Project No. X2008
Task No.
Accession No. DN252022

6. AUTHOR(S)

Cheryl Ann Blain

7. PERFORMING ORGANIZATION NAME(S) AND ADDRESS(ES)

Naval Research Laboratory
Oceanography Division
Stennis Space Center, MS 39529-5004

8. PERFORMING ORGANIZATION REPORT NUMBER

NRL/FR/7322--96-9656

9. SPONSORING/MONITORING AGENCY NAME(S) AND ADDRESS(ES)

Space and Naval Warfare Systems Center
PMW-165
Washington, DC

10. SPONSORING/MONITORING AGENCY REPORT NUMBER

11. SUPPLEMENTARY NOTES

12a. DISTRIBUTION/AVAILABILITY STATEMENT

Approved for public release; distribution unlimited.

12b. DISTRIBUTION CODE

13. ABSTRACT *(Maximum 200 words)*

The Yellow Sea is a very shallow-water body with a strong tidal signal. Its strategic importance had led the U.S. Navy to study tidal response in the Yellow and East China Seas using the Colorado University (CU) data-assimilative, barotropic tidal model. The CU model has been adapted to accept open-ocean boundary forcing from the Grenoble global tidal data base, which is considered more reliable than tides currently obtained from the CU global tidal model. Furthermore, the number and quality of the data assimilation stations utilized by the CU Yellow Sea model is improved. A detailed, semi-automated procedure for assigning data stations for assimilation into the CU model domain has been developed.

Characterization of the tidal elevations in the Yellow and East China Seas from CU model simulations demonstrate that the M_2 constituent is the dominant tidal frequency in the Yellow Sea with amplitudes of nearly 2 m along the coast of west Korea. K_1 is the most significant diurnal component with amplitudes 1/4 of the M_2 tide.

A series of experiments is conducted to test the influence of the location of assimilated data on predictions of the dominant tidal constituents M_2 and K_1. From an analysis of four data station groupings, coastal, shallow, deep, and open boundary located stations, observations located on the continental shelf away from the coastline are most influential in the prediction of primary tides, M_2 and K_1 in the Yellow Sea. Coastal station data may be more influential in the prediction of nonlinear tidal interactions, since these gauges are often located in harbors or inlets where nonlinear tidal interactions are prominent and wave action may be present. Furthermore, coastal data is assimilated into the model at the nearest nodal locations introducing an additional source of error. This examination of the data assimilation component of the CU model should enhance development of data sampling strategies to improve future tidal model predictions.

14. SUBJECT TERMS	15. NUMBER OF PAGES
Yellow Sea, shallow-water modeling, tidal modeling	24
	16. PRICE CODE

17. SECURITY CLASSIFICATION OF REPORT	18. SECURITY CLASSIFICATION OF THIS PAGE	19. SECURITY CLASSIFICATION OF ABSTRACT	20. LIMITATION OF ABSTRACT
Unclassified	Unclassified	Unclassified	Same as report

Validation of the CU tidal model is accomplished by comparing predicted and observed tidal elevations at 49 locations. For eight primary tidal constituents, absolute and root-mean-square (RMS) amplitude and phase errors are examined for data-assimilative and nonassimilative computations. CU model results for the M_2 and K_1 tides are within 13% of measured values, but phases are poorly represented. RMS errors for the data-assimilative simulation are lower than those for the nonassimilative run, but comparison of absolute tidal amplitude errors indicate overdamping by the CU model.

A look at the sensitivity of the bottom friction coefficient specification on model computations shows that the M_2 tide is most affected. An increasing friction coefficient decreases tidal amplitudes, although absolute errors indicate an optimal friction factor between 0.002 and 0.003, which is in good agreement with published values for the Yellow Sea.

CONTENTS

EXECUTIVE SUMMARY

The Yellow Sea is a very shallow-water body with a strong tidal signal. Its strategic importance had led the U.S. Navy to study tidal response in the Yellow and East China Seas using the Colorado University (CU) data-assimilative, barotropic tidal model. The CU model has been adapted to accept open-ocean boundary forcing from the Grenoble global tidal data base, which is considered more reliable than tides currently obtained from the CU global tidal model. Furthermore, the number and quality of the data assimilation stations utilized by the CU Yellow Sea model is improved. A detailed, semi-automated procedure for assigning data stations for assimilation into the CU model domain has been developed.

Characterization of the tidal elevations in the Yellow and East China Seas from CU model simulations demonstrate that the M_2 constituent is the dominant tidal frequency in the Yellow Sea with amplitudes of nearly 2 m along the coast of west Korea. K_1 is the most significant diurnal component with amplitudes 1/4 of the M_2 tide.

A series of experiments is conducted to test the influence of the location of assimilated data on predictions of the dominant tidal constituents M_2 and K_1. From an analysis of four data station groupings, coastal, shallow, deep, and open boundary located stations, observations located on the continental shelf away from the coastline are most influential in the prediction of primary tides, M_2 and K_1 in the Yellow Sea. Coastal station data may be more influential in the prediction of nonlinear tidal interactions, since these gauges are often located in harbors or inlets where nonlinear tidal interactions are prominent and wave action may be present. Furthermore, coastal data is assimilated into the model at the nearest nodal locations introducing an additional source of error. This examination of the data assimilation component of the CU model should enhance development of data sampling strategies to improve future tidal model predictions.

Validation of the CU tidal model is accomplished by comparing predicted and observed tidal elevations at 49 locations. For eight primary tidal constituents, absolute and root-mean-square (RMS) amplitude and phase errors are examined for data-assimilative and nonassimilative computations. CU model results for the M_2 and K_1 tides are within 13% of measured values, but phases are poorly represented. RMS errors for the data-assimilative simulation are lower than those for the nonassimilative run, but comparison of absolute tidal amplitude errors indicate overdamping by the CU model.

A look at the sensitivity of the bottom friction coefficient specification on model computations shows that the M_2 tide is most affected. An increasing friction coefficient decreases tidal amplitudes, although absolute errors indicate an optimal friction factor between 0.002 and 0.003, which is in good agreement with published values for the Yellow Sea.

TIDAL ELEVATIONS IN THE YELLOW AND EAST CHINA SEAS FROM A DATA-ASSIMILATIVE, BAROTROPIC TIDAL MODEL

1.0 INTRODUCTION

Increased interest by the U.S. Navy in the prediction of tides in coastal areas and semi-enclosed seas is a direct result of a shift in emphasis from deep-water, antisubmarine warfare to littoral warfare scenarios. In recent times, the Yellow Sea has grown in strategic importance due to the dynamic political situation between North and South Korea and China and Taiwan, countries whose borders all ring the Yellow and East China Seas. As a consequence, the tidal response in the Yellow and East China Seas is of interest to military planners in the U. S. Navy. The Yellow Sea itself is quite shallow and its circulation is largely dominated by a strong tidal signal. Accurate prediction of the tidal elevation is essential to the success of any military operation in this region.

Implementation of a numerical, barotropic tidal model for any water body involves specification of bathymetry, boundary forcing, and model parameters such as the bottom friction coefficient. Each of the data sources for these model components has associated uncertainties, particularly in coastal areas and marginal seas. Bathymetry is commonly known only to 1/12° and can be inaccurate in near-shore regions. Boundary forcings are taken from sparse data or sea-surface heights, which themselves have been computed from larger scale ocean models. Model parameter selection is often based on experience or values are "tuned" during model calibration.

To partially compensate for uncertainties in model data and overcome errors due to inadequate grid resolution, observed tidal heights are merged with numerical tidal models through data assimilation. In coastal zones and marginal seas where complex bathymetry and irregular shorelines produce highly nonlinear tidal interactions, the assimilation of tidal heights into model computations may significantly improve model performance. Furthermore, for short-term forecasts, the assimilation of observed sea-surface heights on real-time scales may be required to achieve a desired accuracy in computed tidal elevations.

The U. S. Navy currently exercises a relocatable, data-assimilative, barotropic tidal model in the Yellow Sea. This model is the Colorado University (CU) tidal model and is a variant of the Princeton finite difference, hydrodynamic model. The CU model utilizes a coarse grid and relies heavily on data assimilation to achieve accurate tidal predictions (Kantha et al. 1994). In the Yellow and East China Seas, ample observation points are available for assimilation into the tidal model or for comparison during model evaluation. Data sources include tide gauges as well as TOPEX/Poseidon altimeter measurements (Lee-Lueng et al. 1994).

From CU model predictions of tidal elevation, a spatial description of tidal forcing in the Yellow and East China Seas is obtained. Cotidal charts for eight primary tidal constituents are derived and their relative contributions to the overall tidal signal are assessed. The influence of the location of assimilated data on computed sea-surface height predictions for the major semidiurnal, M_2, and diurnal, K_1, tidal constituents is demonstrated. Tidal data located at 114 stations are

divided into four groups corresponding to the bathymetry at their location or their proximity to open-ocean boundaries. Tidal heights computed by assimilating each group of data stations separately are qualitatively compared to assess how differences in the tidal solutions can be attributed to station location. Finally, the CU model capability, with respect to prediction of tidally induced sea-surface height, is quantitatively evaluated. The 114 locations of measured tides are separated into assimilation stations and observational data locations. Absolute and root-mean-square (RMS) errors of model computations derived from comparisons to the observed tidal elevations are presented. As part of this model evaluation, the sensitivity of bottom friction coefficient on model results is briefly considered.

2.0 NUMERICAL MODELING STRATEGY

The hydrodynamic computations are made using a fully nonlinear, two-dimensional, barotropic tidal model developed at CU (Kantha et al. 1994; Kantha 1995). The governing equations are derived from the three-dimensional equations for mass and momentum balance subject to the hydrostatic assumption, the Boussinesq approximation, and vertical integration over the water column. Written in spherical coordinates the equations take the following form:

$$\frac{\partial \eta}{\partial t} + \frac{1}{R^2 \cos\phi}\left[\frac{\partial}{\partial \lambda} RD\overline{u_\lambda} + \frac{\partial}{\partial \phi} R\cos\phi\, D\overline{u_\phi}\right] = 0 \tag{1}$$

$$\frac{\partial}{\partial t} Du_\lambda + \underline{\bar{u}} \cdot \nabla \overline{u_\lambda} - fD\overline{u_\phi} + \frac{\overline{u_\lambda}\,\overline{u_\phi} D\tan\phi}{R} = \tag{2}$$

$$-D\frac{\partial}{\partial \lambda}\left[\frac{p}{\beta} + g(\eta - \alpha\xi)\right] - \tau_{b\lambda} + D\overline{F_\lambda}$$

$$\frac{\partial}{\partial t} D\overline{u_\phi} + \underline{\bar{u}} \cdot \nabla \overline{u_\phi} - fD\overline{u_\lambda} - \frac{\overline{u_\lambda^2} D\tan\phi}{R} = \tag{3}$$

$$-D\frac{\partial}{\partial \phi}\left[\frac{p}{\beta} + g(\eta - \alpha\xi)\right] - \tau_{b\phi} + D\overline{F_\phi},$$

where t represents time, λ, ϕ are degrees longitude (east of Greenwich positive) and degrees latitude (north of the equator positive), η is the free surface elevation relative to the geoid, $\overline{u_\lambda}$, $\overline{u_\phi}$ are the depth-averaged horizontal velocities, R is the radius of the Earth, D is the bathymetric depth relative to the geoid, $f = 2\Omega\sin\phi$ is the Coriolis parameter, Ω is the angular speed of the Earth, p is the atmospheric pressure at the free surface, g is the acceleration due to gravity, β is the reference density of water, $\alpha\xi$ is the effective Newtonian equilibrium tidal potential, $\tau_{b\lambda}$, $\tau_{b\phi}$ are the bottom stresses, and $\overline{F_\lambda}$, $\overline{F_\phi}$ are the horizontal mixing terms.

In the current implementation of the CU model, both baroclinic forcings and wind stress are neglected. Bottom friction terms are parameterized using a quadratic drag law and a Laplacian formulation characterizes the horizontal mixing. The viscosity coefficient in the horizontal mixing

terms is composed of two parts: a constant and a Smagorinsky nonlinear portion, which is dependent on mean strain rate (Smagorinsky 1963).

The equilibrium tidal potential, ξ, which represents astronomical forcing by celestial bodies, the sun and the moon, is taken from Schwiderski (1980):

$$\xi(\lambda,\varphi,t) = \sum_{nij} B_{jn} L_j(\varphi) \cos\,(2\pi t/T_{jn} + j\lambda + \chi_{jn}) , \tag{4}$$

where B_{jn} is the amplitude of constituent n for species j = 0, 1, 2, the corresponding period is T_{jn}, χ_{jn} is the astronomical argument, and $L_j(\varphi)$ is defined by:

$$L_0(\varphi) = 3\,\sin^2\varphi - 1, \tag{5}$$

$$L_1(\varphi) = \sin 2\varphi, \tag{6}$$

$$L_2(\varphi) = \cos^2\varphi. \tag{7}$$

The use of frequency and time-dependent nodal factors is not required by the CU model when using the following methodology. Primary constituents, four semidiurnal (M_2, S_2, N_2, and K_2), four diurnal (K_1, O_1, P_1, and Q_1), and three long-term (Mf, Mm, Ssa), are simulated individually using the CU model. The orthotide approach of Groves and Reynolds (1975) can then be applied to compute the total tidal response, which includes 60 high-frequency components and 15 of the most significant long-term equilibrium tides. The only time-dependent information needed for a model simulation is the date and year. Basis for the orthotide approach lies in the representation of tides as a linear combination of a special set of orthogonal tidal functions. The reader is referred to Groves and Reynolds (1975) or Kantha (1995) for a more complete discussion of the implementation and facility of the orthotide method.

The governing equations are discretized using an explicit, finite difference scheme over an orthogonal, curvilinear grid. The grid is known as the staggered Arakawa-C grid where sea-surface height and velocity are computed at locations within the grid cell that differ by one half the grid spacing. In time, a forward differencing scheme is implemented to reduce stability restrictions on the time step. Numerical formulations in the CU tidal model are nearly identical to that of the well-known Princeton hydrodynamic model (e.g., Blumberg and Mellor 1987; O'Connor 1991).

A distinctive feature of the CU model over other shallow-water models (e.g., Blumberg and Mellor 1987; Lynch and Werner 1991; Luettich et al. 1992) is the assimilation of tidal component data taken from coastal tide gauges and/or altimetry sources. A rather simplistic data-assimilation procedure, nudging, is implemented. Nudging is a localized version of optimal interpolation techniques that are widely used in conjunction with dynamical models having heterogeneous observations (Ghil and Malanotte-Rizzoli 1991). Model predicted sea-surface heights at assimilation locations are replaced at predetermined intervals by a weighted sum of the model prediction and the observed sea-surface height. Weights for the data are determined a priori and are selected to reflect a level of confidence in the accuracy of assimilated observations.

2.1 Upgrades

The CU model has been adapted to accept open-ocean boundary forcing from the Grenoble global tidal data base (LeProvost et al. 1994), which is considered more reliable than tides currently

implemented and obtained from the CU global tidal model (Kantha 1995). The Grenoble tide solutions are derived from a finite element hydrodynamic model. For the M_2 and S_2 tidal constituents, empirically computed tidal heights derived from TOPEX/Poseidon data are assimilated into the model computations for an improved solution. The Grenoble tidal solutions have a resolution down to 10 km along the coasts and the released data base is gridded with a 0.5-deg resolution for convenience.

Using a constructed preprocessor, any or all of eight primary tidal constituents are directly accessed from the Grenoble tidal data base and then interpolated onto open-ocean boundary points associated with the CU model grid. Tidal constituent data along the open-ocean boundaries takes the form of amplitudes and phases and is written in a format that interfaces with the CU model setup.

Another improvement to the CU model is the inclusion of more, high-quality data-assimilation stations in and around the Yellow Sea. A total of 114 locations throughout the Yellow and East China Seas are identified as either having tide gauge observations or TOPEX/Poseidon-derived sea-surface heights. For quality control purposes, the tide gauges included in this group were active for at least 180 days and are extracted from the International Hydrographic Office data (IHO 1979). Altimetric tides are derived from TOPEX data according to Desai and Wahr (1994).

A detailed, semi-automated procedure is created to assign data station locations for assimilation into the CU model domain. Given an assimilation station data file in the form specified by the CU model, domain coordinates in latitude and longitude, grid spacing, and bathymetry, data stations are located with the domain or flagged if they are not in the domain or are located over land. Flagged stations can be manually included as assimilation stations by specifying a nearby nodal location. Other stations, located over water and within the domain, are automatically assigned to the nearest grid point for assimilation.

3.0 YELLOW SEA TIDAL MODEL

The Yellow Sea, depicted in Fig. 1, is a very shallow, semi-enclosed sea bordered by China to the north and west and Korea in the east. The southern Yellow Sea merges into what is known as the East China Sea. As seen in Fig. 1, bathymetry over much of the Yellow Sea is less than 80 m. The 200-m isobath in the East China Sea forms a sill beyond which depths drop sharply to 1000 m. The source of bathymetry is the digital bathymetric data base (DBDB-5) on which a minimum depth of 5 m is imposed to eliminate drying of computational points along the shoreline. The domain selected for these experiments includes both the Yellow and the East China Seas, extending as far south as Taiwan and eastward to the Japanese island, Kyushu. The finite difference computational grid for this domain is rectangular with a relatively coarse, regular spacing of 0.2 deg (~20 km). Of the 6106 computational points, 3557 are over water and considered active.

Eight primary tidal constituents, four semidiurnal (M_2, S_2, N_2, K_2) and four diurnal (K_1, O_1, P_1, Q_1) tides, are the only forcing considered in the Yellow Sea. Recall the modeling strategy is such that each constituent is simulated separately within the tide model. The eight constituents are forced independently on the interior of the domain through the tidal potential term. At the southern and eastern boundaries, values for the tidal constituents are prescribed using results from the Grenoble global tide model (LeProvost et al. 1994). Tidal heights along the Tsushima Strait at the entrance to the Sea of Japan are taken from Kantha (1994).

Model parameters are identical for all experiments unless specified otherwise so that comparisons between model simulations is possible. The bottom friction coefficient is uniform and equal to

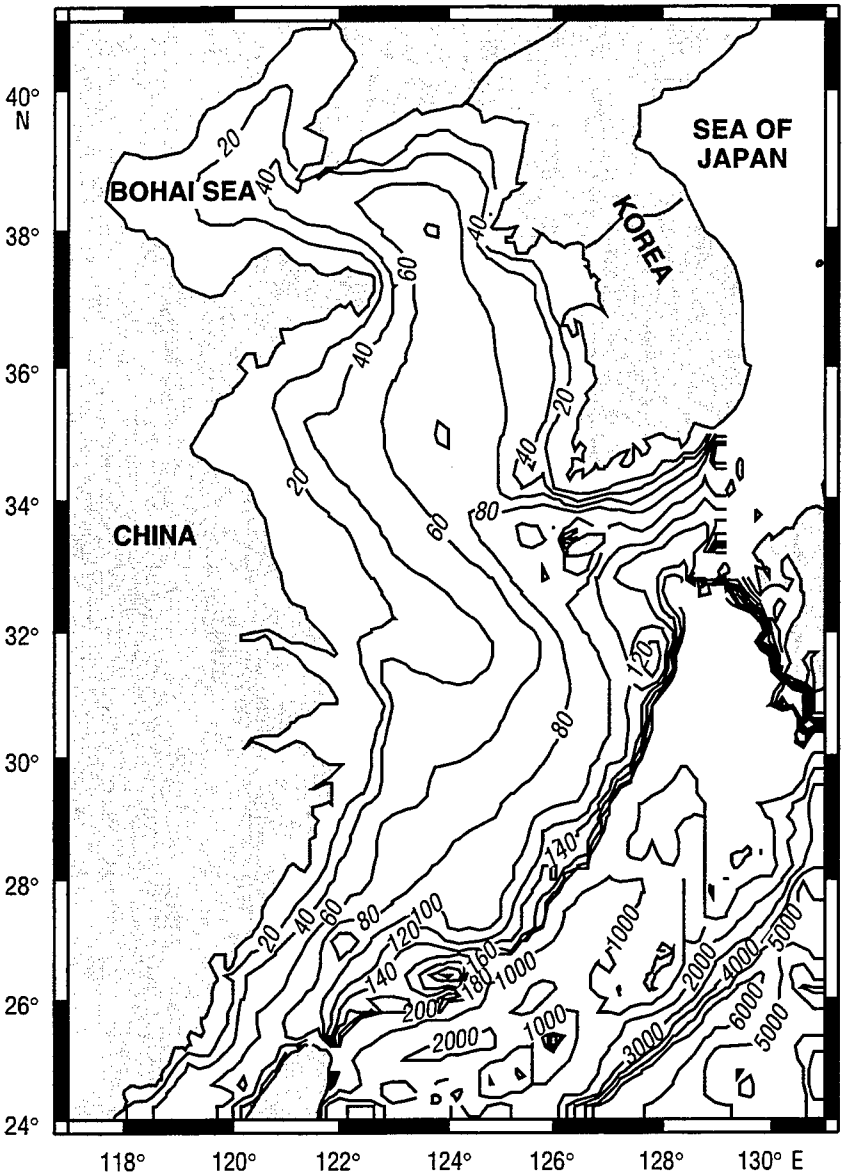

Fig. 1 — Bathymetry contours at 20-m intervals in the Yellow and East China Seas

0.002 for all model runs unless otherwise indicated. The constant part of the horizontal viscosity coefficient has a value of 0.02 and the nonlinear portion associated with the Smagorinsky formulation is specified as 100 m^2/s. Simulations are spun up from a homogeneous initial condition using a ramp in time equivalent to five inertial periods. Model computations proceed for a total of 10 days using a time step of 24 s. Long-term simulations of 150 days produce cotidal charts identical to those computed using 10 days of computation.

A total of 114 locations throughout the Yellow and East China Seas are identified as either having tide gauge observations or TOPEX/Poseidon-derived sea-surface heights. For quality control purposes, the tide gauges included in this group were active for at least 180 days and are extracted from the International Hydrographic Office (IHO) data (IHO 1979). Altimetric tides are derived from TOPEX data according to Desai and Wahr (1994).

4.0 TIDAL ELEVATIONS IN THE YELLOW SEA

Two CU tidal model simulations compute the amplitudes and phases of eight major tidal constituents, M_2, S_2, N_2, K_2 and K_1, O_1, P_1, Q_1, in the Yellow and East China Seas. The first, denoted Run A, includes the assimilation of observed tidal heights at 65 stations, whereas the second, Run NA, includes no data assimilation. In general, tides in the Yellow Sea are influenced by lateral boundaries and depths less than 200 m. Tidal waves propagate from the deep sea onto the continental shelf where they are amplified along the west Korean coast and distorted upon entering the Bohai Sea. Tidal amplitudes in the East China Sea tend to decrease in a direction towards the Sea of Japan.

Mean amplitudes, calculated over all active node points, of all eight major tidal components from model simulations A and NA, are presented in Table 1. The semidiurnal M_2 tide dominates the tidal response in the Yellow Sea. The second-largest contribution to the tidal signal comes from the S_2 tidal frequency, which has magnitudes ranging from 39–46% of the M_2 tidal amplitude. Amplitudes of the strongest diurnal component, K_1, are slightly greater than 1/4 of those associated with the M_2 constituent. The five remaining semidiurnal and diurnal constituents comprise a comparatively small part of the overall tidal amplitude in the Yellow Sea.

When no data is assimilated (Run NA), model-predicted tidal heights are generally larger as reflected in the greater mean amplitude when compared to that of Run A. However, for both simulations NA and A, the relative magnitudes between each of the eight tidal constituents remain stable with only some variation in the S_2 and N_2 magnitudes.

Cotidal charts for the dominant semidiurnal and diurnal tides, M_2 and K_1, are shown in Figs. 2 and 3. While not shown, cotidal charts for the remaining six semidiurnal and diurnal tides exhibit similar patterns as those for M_2 and K_1, respectively. These charts, derived from Run A model computations, include the assimilation of tidal data at 65 locations (shown later in Fig. 7). The M_2 frequency has four amphidrome locations or points of zero amplitude from which tidal phase lines radiate as shown by the dotted lines in Fig. 2. Extreme values of the M_2 tide are nearly 200 cm along the west Korean coast.

For the K_1 tidal component, two amphidromes are evident in dotted phase lines plotted in Fig. 3. Again, tidal heights for K_1 are slightly greater than 1/4 of those associated with M_2 and maximum amplitudes of nearly 40 cm are computed on the west coast of Korea and in the Bohai Sea. These regions of tidal amplification are similar to those seen in the M_2 cotidal chart. In addition, both the amplitudes of M_2 and K_1 are large near the outflow of the Yangtze and Yellow Rivers on the Chinese coast. Qualitative comparisons of the cotidal charts in Figs. 2 and 3, derived from CU model results for M_2 and K_1, with previously published cotidal charts in the Yellow Sea (e.g., Kang et al. 1990; Choi 1984), indicate good agreement.

Table 1 — Mean Amplitudes (m) for Eight Primary Tidal Constituents

RUN	M_2	S_2	N_2	K_2	K_1	O_1	P_1	Q_1
NA	0.7804	0.3589	0.1981	0.0912	0.2188	0.1943	0.0775	0.0453
A	0.7769	0.3011	0.1161	0.1010	0.2165	0.1696	0.0765	0.0343

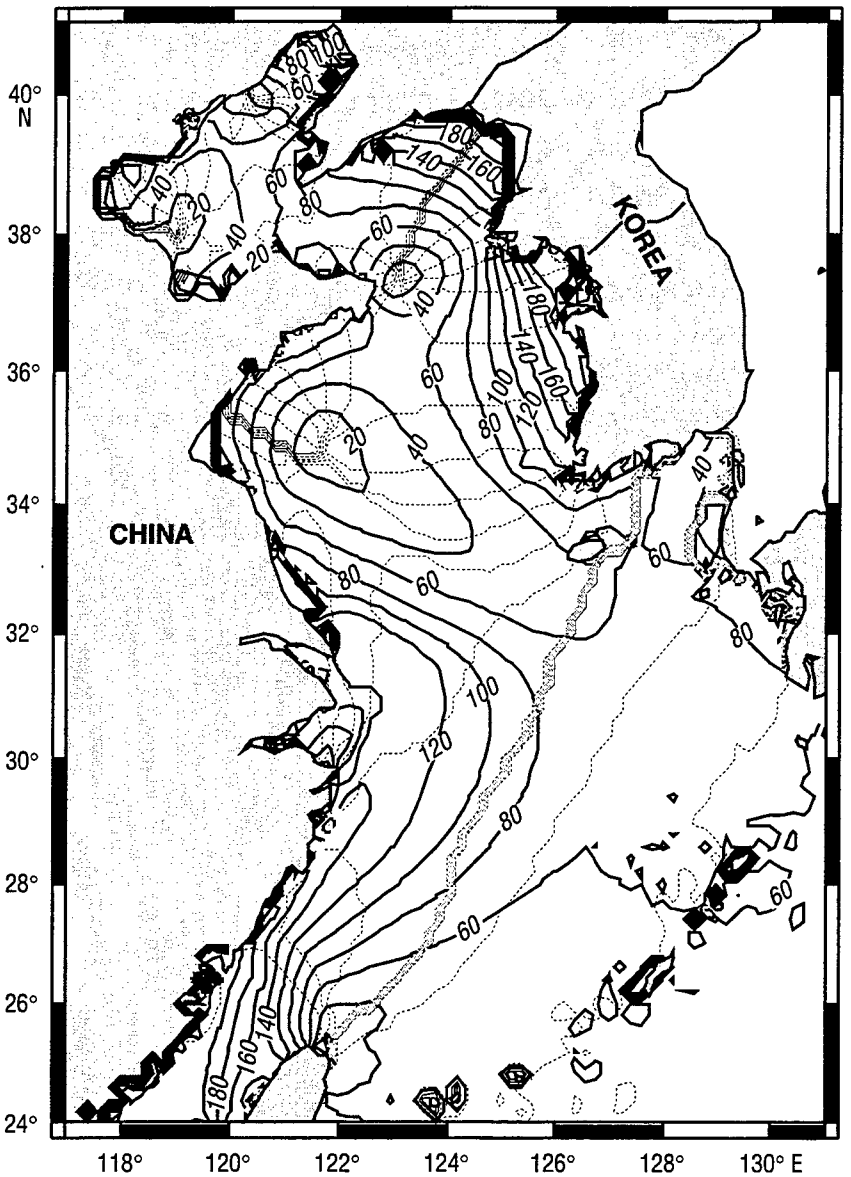

Fig. 2 — Cotidal chart of the M_2 frequency in the Yellow and East China Seas. Amplitudes shown as solid lines at 20-m intervals and dotted lines indicate phases every 30 deg.

5.0 INFLUENCE OF DATA-ASSIMILATION STATION LOCATION

5.1 Experiments

Both TOPEX/Poseidon altimeter and tide gauge data are available in the Yellow and East China Seas and can be assimilated into the CU tidal model. A series of experiments has been designed to test the influence of the location of assimilated data on predictions of the dominant tidal constituents M_2 and K_1. The role of data assimilation in the CU model is assessed to facilitate setup of the model in other regions and to assist in the evaluation of tidal computations. Ideally, one would like to obtain reasonable tidal predictions using the least amount of information a priori.

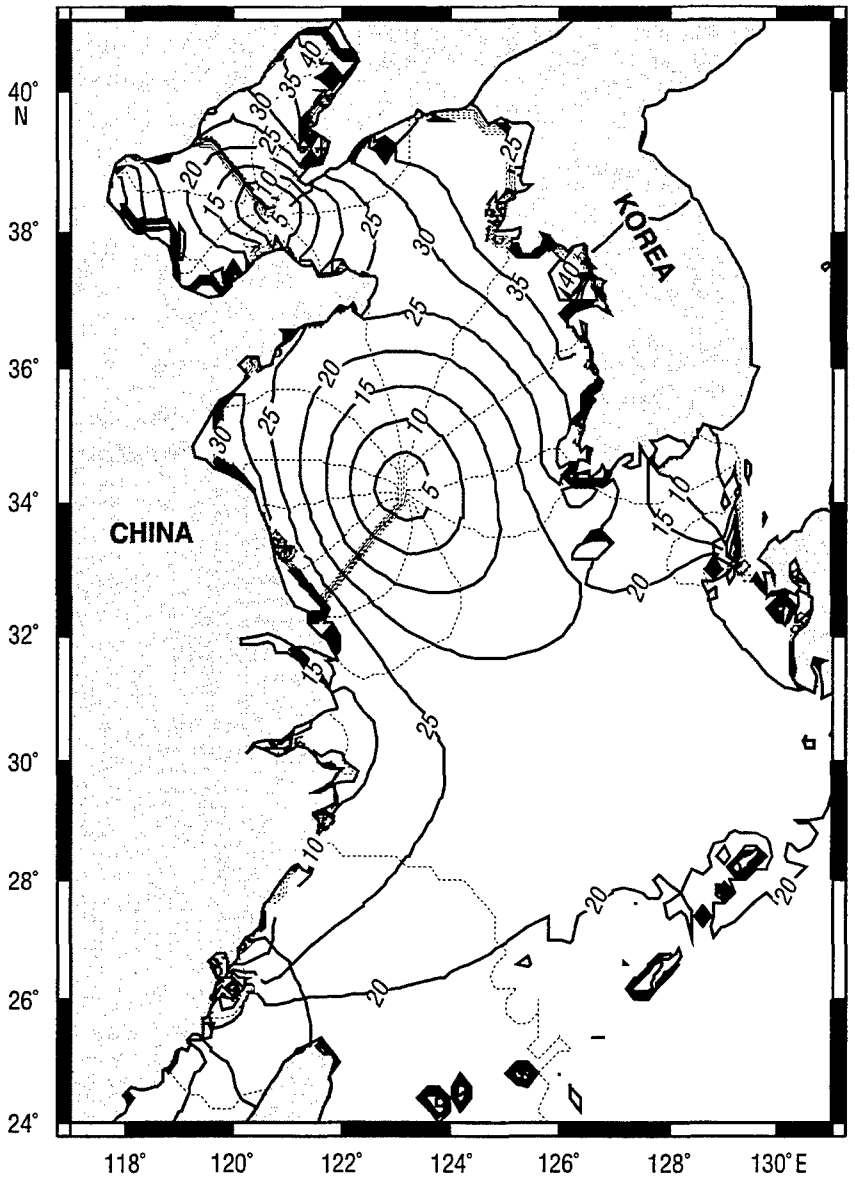

Fig. 3 — Cotidal chart of the K_1 frequency in the Yellow and East China Seas. Amplitudes shown as solid lines at 5-m intervals and dotted lines indicate phases every 30 deg.

Tidal data located at 114 stations are divided into four groups delineated by their location's bathymetry and/or proximity to the open boundaries, shown in Fig. 4, and named accordingly: coastal, shallow, deep, and boundary stations. Coastal stations are those stations that lie along the shoreline. These stations are most likely to record highly localized, nonlinear tidal phenomena. Shallow stations are those stations located offshore in water of depths less than 200 m. Data stations whose water depth is greater than 200 m are categorized as deep stations. Observations that lie closest to the southern, eastern, and Tsushima Strait open-ocean boundaries fall into the boundary station group. Note that each of the stations in the boundary group is taken from one of the three coastal, shallow, or deep station groupings. Table 2 summarizes the number of stations and distinguishing location of the station groupings.

Table 2 — Characteristics of the Location of Assimilated Data

STATION GROUP TYPE	TOTAL NUMBER OF STATIONS	RELATIVE LOCATION
All	114	———
Coastal	51	shoreline (2 m or less)
Shallow	38	2 m < depth < 200 m
Deep	25	depth > 200 m
Boundary	17	near open boundaries

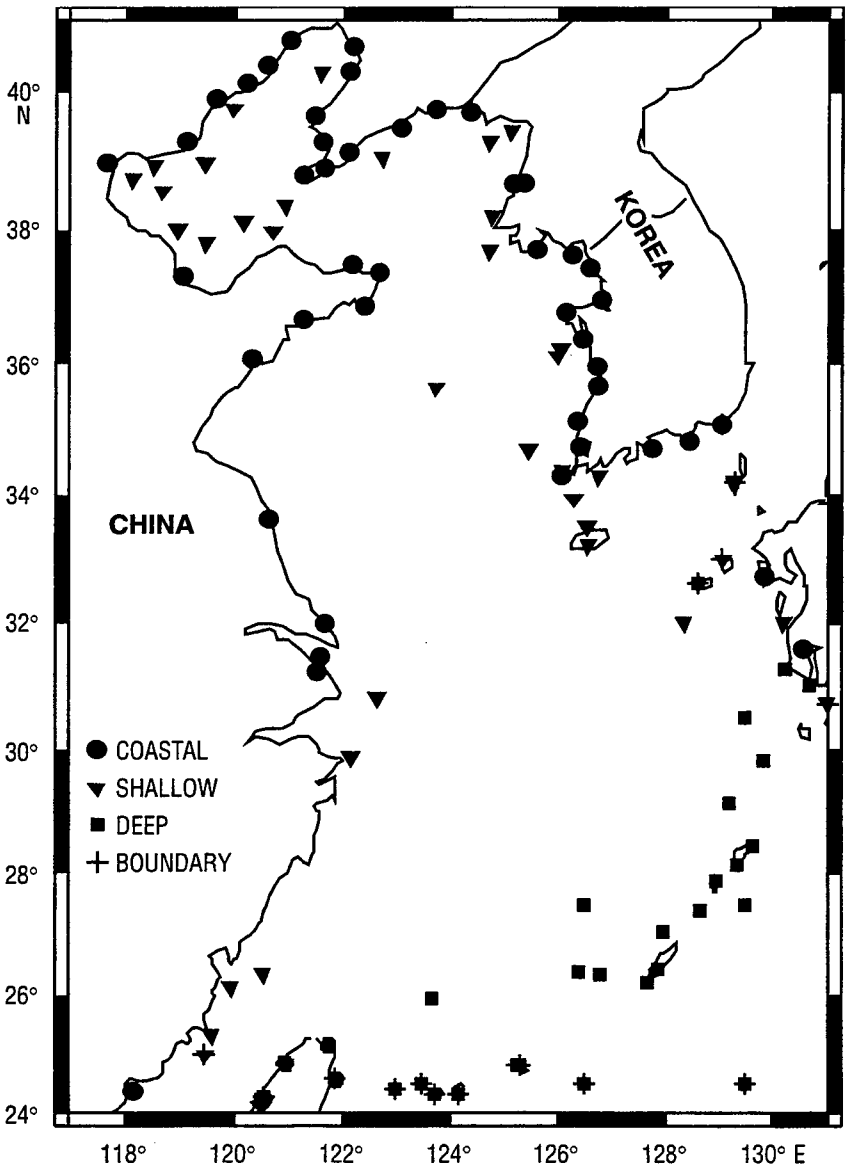

Fig. 4 — Four data assimilation station groupings—coastal, shallow, deep, and boundary—located throughout the Yellow and East China Seas

Six model simulations are conducted for both the M_2 and K_1 tidal constituents with assimilation of either none, all, coastal, shallow, deep, or boundary stations. Cotidal charts for each of the model experiments are constructed and differences in the co-amplitudes between tidal heights obtained by assimilating each of the station groupings are examined to determine if one location is more influential in the computation of primary tides than another.

5.2 Discussion of Results

The contour maps of Fig. 5b–d show deviations between the amplitude of the M_2 tide obtained by assimilation of all observations (Fig. 5a) and amplitudes computed by assimilating deep, shallow, or coastal data stations. Positive values (solid lines) indicate an overprediction and negative values (dotted lines) an underprediction, with respect to the "all-station" case (Fig. 5a). In Fig. 5b, the largest discrepancies in predicted tides occur in the mid-Yellow Sea, along the east and west lateral boundaries, at the northernmost bay in the Bohai Sea, and in the Taiwan Strait. In all of these areas except the upper Bohai Sea and the Taiwan Strait, underprediction is dominant and ranges between 20 to 60 cm. Overprediction at the southern end of the Yellow Sea results from a southeast shift in the amphidrome position. When only those stations designated as boundary station data in Fig. 4 are assimilated, the pattern of differences closely follows that of the deep station assimilation, except overprediction at the Taiwan Strait and underprediction at the Tsushima Strait are somewhat reduced. Noticeable improvements result from the assimilation of a single observation in each of these straits.

Tidal heights for M_2 computed using only shallow observations, as shown in Fig. 5c, differ only slightly from the solution obtained when all data stations are assimilated. Small deviations occur near the Yangtze River, in isolated near-shore regions along the west Korean coast, and in the very shallow upper Bohai Sea. Shallow observations near the Taiwan and Tsushima Straits are included in the data assimilation and, thus, account for the minimal differences seen at these open boundaries. Small differences between predicted M_2 tidal elevations using all stations versus only shallow stations indicate that assimilation of shallow observations dominate computation of the M_2 tidal constituent.

The assimilation of only coastal station data into computations of the M_2 tide produces large variations of the M_2 amplitude in the upper Yellow Sea seen in Fig. 5d. In particular, excessive underprediction, up to 60 cm, is located offshore from the Chinese border. Within the Bohai Sea itself differences are relatively small. Coastal stations bounding the Taiwan Strait fail to constrain M_2 elevations in that region. Generally, the M_2 tide computed in shallow regions away from the coastline does not agree with elevations obtained when all stations are assimilated. Coastal stations may not be as effective in predicting the M_2 tide in part because stations are located in the very nearshore, outside the domain modeled due to the minimum bathymetry specification of 5 m. Furthermore, coastal stations capture highly nonlinear, localized behavior near inlets and harbors and may not be well-suited to the prediction of primary tides.

Similarly, for the K_1 tidal constituent, contour maps in Fig. 6b–d show differences in tidal elevation computed using each of the data-assimilation groups, deep, shallow, and coastal, as compared to the K_1 solution obtained from an assimilation of all stations (Fig. 6a). Again, overprediction is indicated as a solid line and underprediction by a dotted line. As shown for the M_2 tide, independent assimilation of the deep and boundary station data yields interchangeable results. The most significant differences in tidal height predictions in comparison to the all-data-assimilation case are concentrated in the far upper Yellow Sea, seen in Fig. 6b. Magnitudes of the differences lie in the

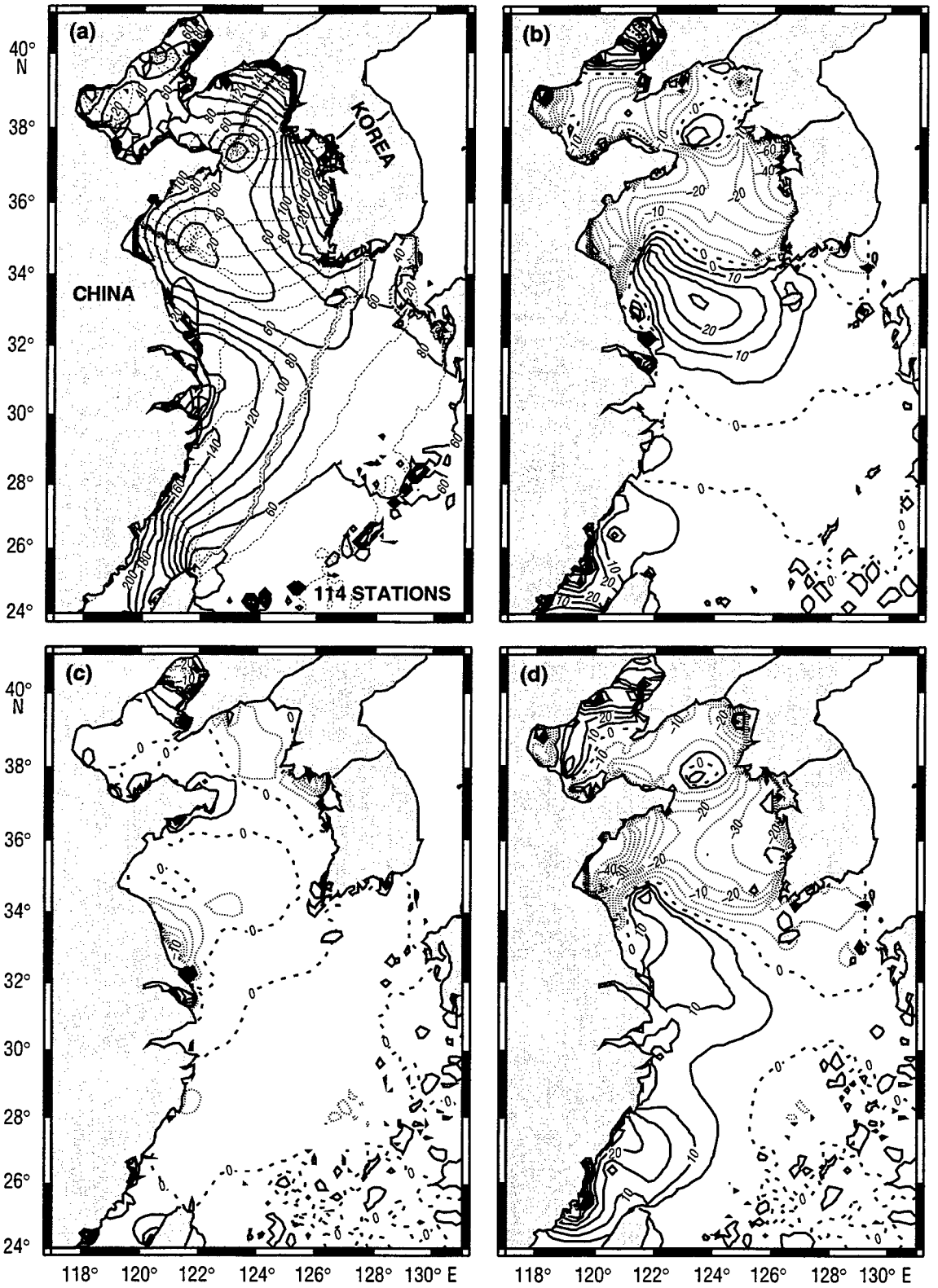

Fig. 5 — (a) Cotidal chart of the M_2 tide with amplitudes in 20-cm solid contours and phases in dotted lines at 30-deg intervals. Differences between the M_2 amplitude computed by assimilating all data stations and only (b) deep stations, (c) shallow stations, or (d) coastal stations. Contours are plotted at 5-cm intervals with overprediction (positive) as solid lines and underprediction (negative) as dotted lines.

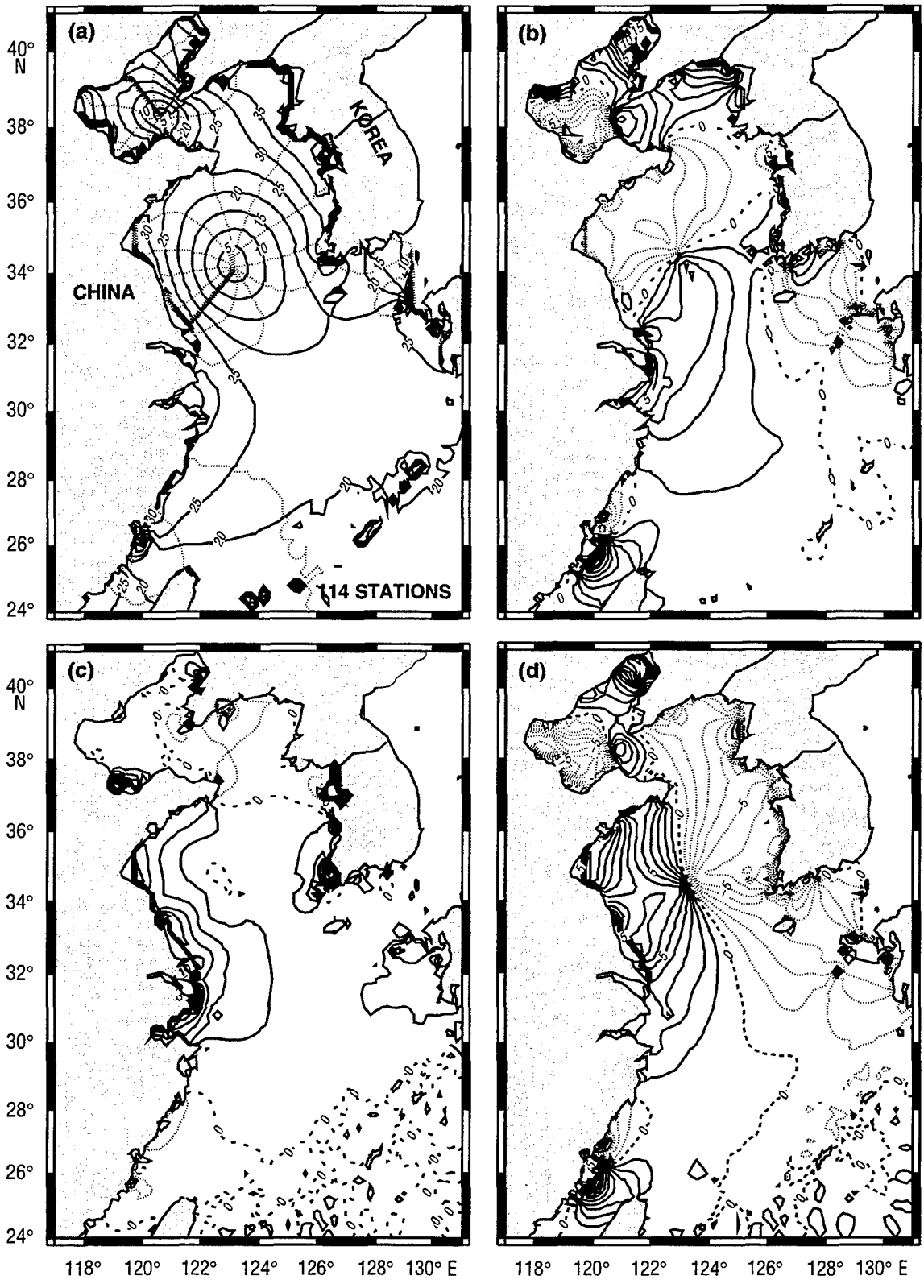

Fig. 6 — (a) Cotidal chart of the K_1 tide with amplitudes in 5-cm solid contours and phases in dotted lines at 30-deg intervals. Differences between the K_1 amplitude computed by assimilating all data stations and only (b) deep stations, (c) shallow stations, or (d) coastal stations. Contours are plotted at 1-cm intervals with overprediction (positive) as solid lines and underprediction (negative) as dotted lines.

range of 8 cm or less with exceptions in the northern Bohai sea, at the Yangtze River entrance, at Incheon on the South Korean coast, and in the Taiwan Strait where differences reach up to 20 cm.

The assimilation of shallow observations results in a solution for K_1 that closely mirrors that obtained by assimilation of all observations as shown in Fig. 6c. Locations near Incheon and the Yangtze River offer the only major discrepancies. Again, the assimilation of shallow data dominates the computed tidal solution, in this case for the K_1 tide.

The assimilation of coastal station data leads to a distinctive over- and underprediction north-south division in the Yellow Sea as depicted in the difference map of Fig. 6d. Underprediction is indicated along the west Korean coast and overprediction along the Chinese coast. This pronounced feature can be attributed to a shift in the centrally located amphidrome in the K_1 tide. Magnitudes of the differences remain less than 10 cm except at points near the Taiwan Strait, on the Chinese coast, an in the extremely shallow regions of the Bohai Sea.

Tidal predictions for K_1, which independently assimilate the four designated groups of data stations, exhibit only small changes between them as compared to the larger differences associated with computations of the M_2 tide using each of the station groupings.

5.3 Conclusions

The assimilation of data into the CU tidal model is influential in predicting the tidal response of the Yellow Sea basin. From an analysis of four data station groupings, coastal, shallow, deep, and open boundary located stations, observations located on the continental shelf away from the coastline are most influential in the prediction of primary tides, M_2 and K_1, in the Yellow Sea. Effects of deep-water stations or those located near large, open-ocean boundaries do not reach beyond the deeper waters and have little impact on tidal computations on the continental shelf. However, the analysis here has shown that tidal data assimilated in the open water of narrow straits can improve local tidal height computations. The influence of coastal station data was largest in small near-shore regions and was not a major factor in the computation of the primary tides, M_2 and K_1. Coastal gauges are often located in harbors or inlets where nonlinear tidal interactions are prominent and wave action may be present, a phenomena not included in the model physics. A preliminary examination of the M_4 overtide solution (not shown) indicates that assimilation of coastal observations may be more significant in predicting nonlinear tidal patterns in the northern Yellow Sea. A thorough look at the role of data assimilation in the prediction of nonlinear tidal constituents is slated for future study.

This documentation of CU model performance should enhance development of data sampling strategies to improve future tidal model predictions. Issues of how often to assimilate data or how to assign appropriate weights to each observation are not addressed here.

6.0 TIDAL MODEL EVALUATION

From the original 114 data locations in the Yellow Sea (Fig. 4), 49 points are selected to serve as measurements against which tidal model computations are evaluated. These observation locations, depicted in Fig. 7, are selected so that their spatial distribution covers much of the Yellow and East China Seas model domain. At the remaining 65 locations, also shown in Fig. 7, measured tidal heights are assimilated into tidal model computations at each time step, intervals of 24 s.

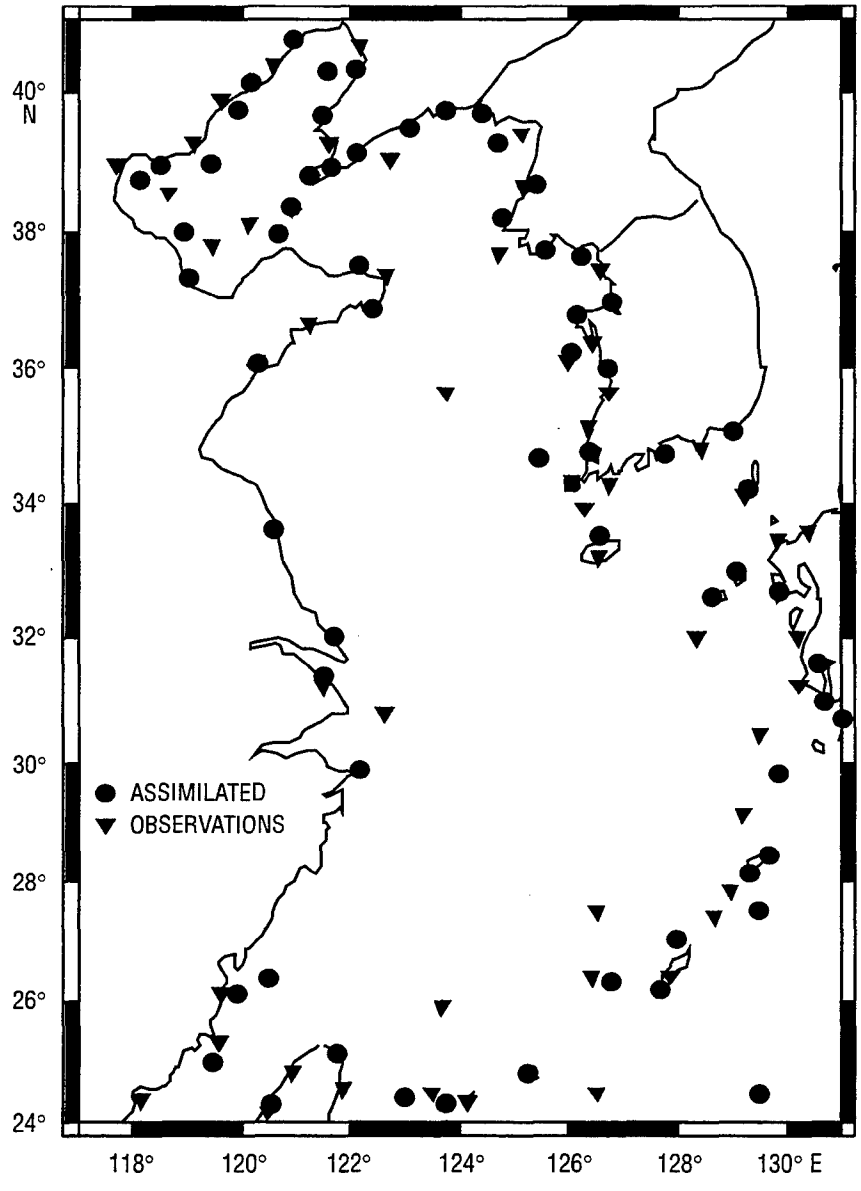

Fig. 7 — Locations of 65 data-assimilation stations and 49 observational points for tidal elevation in the Yellow and East China Seas

Tidal elevations are assimilated as amplitudes and phases of each tidal constituent. Weights assigned to the stations are fixed at 90%.

The CU tidal model is evaluated by comparing computations of the amplitudes and phases of eight major tidal constituents, M_2, S_2, N_2, K_2 and K_1, O_1, P_1, Q_1, to measured tidal amplitudes and phases at the 49 measurement locations throughout the Yellow and East China Seas. For components N_2, K_2, P_1, and Q_1, observations are only available at 20, 17, 21, and 12 of the 49 measurement locations, respectively. Two simulations, Run A and Run NA mentioned previously, are conducted for this model evaluation. Recall Run A includes the assimilation of observed tidal heights at 65 stations, whereas Run NA has no data assimilation.

6.1 Comparison to Observations

From Foreman (1993), differences between model-derived and measured tidal amplitudes and phases are computed as distances, D, in the complex plane:

$$D = \{(A_o \cos P_o - A_m \cos P_m)^2 + (A_o \sin P_o - A_m \sin P_m)^2\}^{1/2}, \quad (8)$$

where A_o, A_m, P_o, and P_m are the observed and modeled amplitudes and phases, respectively. Average values of D for each tidal constituent, as well as average differences between model computed and observed amplitudes and phases, are given in Table 3 for Run A, the data-assimilative simulation. From Table 3, the average M_2 amplitude error is approximately 13 cm and the distance in the complex plane is nearly 30 cm, a significant portion of which is due to large phase errors. Though the largest discrepancies between model results and observations occur in the prediction of the M_2 tide, as measured by D, proportionally, the differences in amplitude for M_2 and K_1 are less than 13% of mean measured amplitudes for these constituents. Model performance is considerably worse for the four less prominent tidal frequencies, N_2, K_2, P_1, and Q_1, and may be due in part to the reduced number of measurement points available for comparison.

Spatially, the most significant differences between model computed and observed tidal amplitude and phase are concentrated along the west coast of Korea and in the Taiwan Strait. Near Incheon, located on the northwest South Korean coast, tide model results are extremely poor in comparison to observed values. The complex coastline and very shallow depths at Incheon are not well represented by the coarse CU Yellow Sea model and largely account for the significant disparity. Some errors in the shallowest water may be attributed to coastal gauges located in harbors or inlets where nonlinear tidal interactions are prominent and wave action may be present, a phenomena not included in the model physics. Furthermore, coastal data is assimilated into the model at nearest nodal locations introducing an additional source of error.

In the deep waters, particularly those locations where TOPEX/Poseidon altimetry data has been assimilated, model predictions are quite good. Tidal data assimilated in open waters of narrow straits improves local tidal height computations. Deep-water assimilation of data has little impact on tidal predictions on the continental shelf.

Table 3 — Absolute Errors from Run A for Eight Primary Tidal Constituents

ABSOLUTE ERRORS	M_2	S_2	N_2	K_2	K_1	O_1	P_1	Q_1
D, m	0.290	0.153	0.101	0.083	0.064	0.052	0.033	0.027
$\lvert A_o - A_m \rvert$, m	0.126	0.071	0.061	0.066	0.031	0.028	0.026	0.16
$\lvert P_o - P_m \rvert$, deg	46.18	82.16	38.66	76.02	26.48	12.11	28.01	31.37
Measured Mean Amplitude	0.9880	0.3471	0.1836	0.1134	0.2606	0.1955	0.0773	0.0336

Finally, RMS errors are computed for each major constituent using the standard formula:

$$RMS_i = \left\{ \left(\sum_n (t_m - t_o)_i^2 \right) / n \right\}^{1/2}, \tag{9}$$

where i is the tidal constituent, t_m, t_o are the model and observed amplitudes or phases, and n is the number of observation points. RMS errors computed for Runs NA and A are presented in Table 4a for amplitude and in Table 4b for phase. A one- to two-fold reduction in the RMS error is evident in tidal amplitudes computed using a data-assimilative model, i.e., Run A, as compared to the no assimilation case, Run NA.

RMS amplitude errors represented as a percentage of the mean measured amplitude of each constituent are also given in Table 4a. For Run A, the lowest percentage RMS errors for amplitude, 17–19%, are linked to the diurnal tidal constituents K_1 and O_1. Semidiurnal components M_2 and S_2 have proportional RMS amplitude errors ranging from 30–40%. Significantly larger RMS percentage amplitude errors are computed for remaining constituents and may again be a consequence of fewer observational points available for comparison. RMS phase errors are noticeably poor with an RMS phase difference just over 110° for the M_2 tide and nearly 87° for the K_1 tide.

6.2 Sensitivity of Bottom Friction Coefficient

Table 5 shows the effect of varying c_f on mean tidal amplitudes, as well as RMS and absolute errors of amplitude and phase, for the major semidiurnal and diurnal frequencies, M_2 and K_1. Selected friction factors in the range from 0.0005 to 0.004 are fixed over the entire Yellow and East China Seas model domain. An increase in the friction factor most notably affects model computations of amplitude and phase for the M_2 tidal constituent. The mean M_2 amplitudes and RMS amplitude errors decrease with increasing c_f values and are reduced by approximately 10 and 12%, respectively, over the range of friction factors considered. RMS phase errors computed for each friction coefficient are within 10° with a minimum occurring at $c_f = 0.002$.

Table 4a — RMS Amplitude Errors (m) for Eight Primary Tidal Constituents

RUN	M_2	S_2	N_2	K_2	K_1	O_1	P_1	Q_1
NA	0.4493	0.2604	0.1440	0.1133	0.0748	0.0788	0.0519	0.0516
A	0.2989	0.1331	0.0996	0.1093	0.0439	0.0363	0.0551	0.0285
% of Obs.	30	38	54	96	17	19	71	85

Table 4b — RMS Phase Errors (deg) for Eight Primary Tidal Constituents

RUN	M_2	S_2	N_2	K_2	K_1	O_1	P_1	Q_1
NA	136.33	141.21	83.00	137.02	71.90	71.37	99.06	54.20
A	110.31	151.82	83.54	142.50	86.91	49.35	105.43	41.89

Table 5a — Run A Statistics for the M_2 Tide Under a Varying Friction Factor

FRICTION FACTOR, c_f	MEAN AMP, m	RMS ERRORS AMP, m	RMS ERRORS PHASE, deg	D, m	$\lvert A_o - A_m \rvert$ m	$\lvert P_o - P_m \rvert$ deg
0.0005	0.8282	0.2916	121.04	0.291	0.169	52.33
0.001	0.8056	0.2515	121.93	0.279	0.148	52.74
0.002	0.7769	0.2040	110.59	0.290	0.126	46.18
0.003	0.7574	0.1851	111.09	0.285	0.115	46.19
0.004	0.7418	0.1817	112.28	0.287	0.116	46.89

Table 5b — Run A Statistics for the K_1 Tide Under a Varying Friction Factor

FRICTION FACTOR, c_f	MEAN AMP, m	RMS ERRORS AMP, m	RMS ERRORS PHASE, deg	D, m	$\lvert A_o - A_m \rvert$ m	$\lvert P_o - P_m \rvert$ deg
0.0005	0.2162	0.0622	72.33	0.080	0.040	26.86
0.001	0.2159	0.0463	75.12	0.069	0.034	26.94
0.002	0.2165	0.0435	76.17	0.064	0.031	26.48
0.003	0.2165	0.0428	76.82	0.062	0.031	26.53
0.004	0.2162	0.0423	77.05	0.060	0.031	26.46

The varying bottom friction coefficient effects the K_1 frequency to a much lesser extent. K_1 mean amplitudes remain close in magnitude, changing less than 0.2%, and exhibit no clear trend in relation to the friction factor specification. In contrast, RMS amplitude errors computed for the K_1 tide decrease with increasing c_f values and RMS phase errors exhibit the reverse. Keep in mind that these deviations in model computations of the K_1 tide in response to changing friction coefficients are slight. The ratio of M_2 to K_1 amplitudes is relatively stable, changing by only 3%, regardless of the bottom friction factor selected.

Absolute error measures in Table 5 echo the M_2 RMS amplitude error trend that differences decrease for increasing values of c_f. Again, changes in errors associated with the M_2 tide are more dramatic than those of the K_1 tide. Amplitude and phase absolute error measures for M_2 and K_1 tidal frequencies, for the most part, reach a minimum when the bottom friction factor is in the range of 0.002–0.003. These c_f values correspond to $c_f = 0.0025$, a value most often reported in the literature for Yellow Sea tidal simulations (i.e., Kang et al. 1990; Lee and Beardsley 1993; Zhenxing et al. 1994).

6.3 Conclusions

An evaluation of the CU tidal model computations for eight primary tidal constituents demonstrates that the assimilation of data into tidal models can be influential in predicting the tidal response of a basin. A coarse tidal model of the Yellow Sea produces reasonable computations of tidal elevation with low RMS errors when compared at 49 observation sites. RMS errors derived from CU model

simulations of tidal elevation computed with and without data assimilation indicate that assimilation of tidal information reduces error by a factor of two. An abundance of reliable sea-surface height observations from coastal stations and satellite sources in the Yellow Sea partially compensates for the coarse grid resolution of the CU tidal model.

The M_2 tidal constituent is the dominant frequency in the Yellow Sea. Amplitudes reach nearly 2 m along the coast of west Korea. K_1 is the most significant diurnal component with amplitudes just over 1/4 of those for the M_2 tide. Computed amplitudes of the M_2 and K_1 tides are within 13% of measured tidal elevations at 49 locations. Phases computed by the CU Yellow Sea tidal model are poorly represented and warrant further investigation. Additional improvements would no doubt result from using a more highly resolved grid discretization.

A sensitivity study of bottom friction coefficient specification on model results suggests the friction factor is most influential in computations of the M_2 tide. As expected, an increasing friction coefficient decreases tidal amplitudes. Absolute errors reveal an optimal friction coefficient ranging between 0.002 and 0.003, values that agree well with published numbers for the Yellow Sea.

Generally, tidal amplitudes for all eight constituents computed using data assimilation are overdamped. This overdamping of the tidal amplitude may be the result of numerical deficiencies in the model or inappropriate specification of the horizontal mixing parameter, since the bottom friction coefficient has been shown to have limited influence. Issues of how often to assimilate data or how to assign appropriate weights to each observation are not addressed here. Nonlinear tidal interactions have been ignored in this paper but are the focus of current studies using the CU Yellow Sea tidal model.

7.0 SUMMARY

The Yellow Sea is a very shallow-water body with a strong tidal signal. Its strategic importance had led the U. S. Navy to study tidal response in the Yellow and East China Seas using the Colorado University data-assimilative, barotropic tidal model. The CU model has been adapted to accept open-ocean boundary forcing from the Grenoble global tidal data base, which is considered more reliable than tides currently obtained from the CU global tidal model. Furthermore, the number and quality of the data-assimilation stations utilized by the CU Yellow Sea model is improved. A detailed, semi-automated procedure for assigning data stations for assimilation into the CU model domain has been developed.

Characterization of the tidal elevations in the Yellow and East China Seas from CU model simulations demonstrate that the M_2 constituent is the dominant tidal frequency in the Yellow Sea with amplitudes of nearly 2 m along the coast of west Korea. K_1 is the most significant diurnal component with amplitudes 1/4 of the M_2 tide.

A series of experiments is conducted to test the influence of the location of assimilated data on predictions of the dominate tidal constituents, M_2 and K_1. From an analysis of four data station groupings, coastal, shallow, deep, and open boundary located stations, observations located on the continental shelf away from the coastline, are most influential in the prediction of primary tides, M_2 and K_1, in the Yellow Sea. Coastal station data may be more influential in the prediction of nonlinear tidal interactions since these gauges are often located in harbors or inlets where nonlinear tidal interactions are prominent and wave action may be present. Furthermore, coastal data is assimilated into the model at the nearest nodal locations introducing an additional source of error.

This examination of the data-assimilation component of the CU model should enhance development of data sampling strategies to improve future tidal model predictions.

Validation of the CU tidal model is accomplished by comparing predicted and observed tidal elevations at 49 locations. For eight primary tidal constituents, absolute and RMS amplitude and phase errors are examined for data-assimilative and nonassimilative computations. CU model results for the M_2 and K_1 tides are within 13% of measured values, but phases are poorly represented. RMS errors for the data-assimilative simulation are lower than those for the nonassimilative run, but comparison of absolute tidal amplitude errors indicate overdamping by the CU model.

A look at the sensitivity of the bottom friction coefficient specification on model computations shows that the M_2 tide is most affected. An increasing friction coefficient decreases tidal amplitudes although absolute errors indicate an optimal friction factor between 0.002 and 0.003, which is in good agreement with published values for the Yellow Sea.

8.0 ACKNOWLEDGMENTS

This work was funded through the Office of Naval Research's Navy Ocean Modeling and Prediction Program (Program Element 0602435N). Thanks are extended to Dr. L. Kantha for his assistance and use of the CU tidal model.

9.0 REFERENCES

Blumberg, A. F. and G. L. Mellor, "A Description of a Three-Dimensional Coastal Ocean Circulation Model," in *Three Dimensional Coastal Ocean Models*, N. S. Heaps, ed. (AGU Press, Washington, D.C., 1987), pp. 1–16.

Choi, B. H., "A Three-Dimensional Model of the East China Sea," in *Ocean Hydrodynamics of the Japan and East China Seas*, T. Ichiye, ed. (Elsevier, 1984), pp. 209–224.

Desai, S. D. and J. M. Wahr, "Another Ocean Tide Model Derived from TOPEX/Poseidon Satellite Altimetry," (abstract) *EOS* **75**(57), 1994.

Foreman, M. G. G. and R. F. Henry, "A Finite Element Model for Tides and Resonance Along the North Coast of British Columbia," *J. Geophys. Res.* **98**(C2), 2509–2531 (1993).

Ghil, M. and P. Malanotte-Rizzoli, "Data Assimilation in Meteorology and Oceanography," *Advances in Geophysics* **33**, 141–266 (1991).

Groves, G. W. and R. W. Reynolds, "An Orthogonalized Convolution Method of Tide Prediction," *J. Geophys. Res.* **80**, 4131–4138 (1975).

International Hydrographic Office, "Tidal Constituent Bank, Station Catalogue, Ocean and Aquatic Sciences," Dept. of Fisheries and Oceans, Ottawa, Canada, 1979.

Kang, S. K., S.-R. Lee, and K.-D. Yum, "Tidal Computation of the East China Sea, the Yellow Sea, and the East Sea," in *Oceanography of Asian and Marginal Seas*, A. Takano, ed. (Elsevier, 1990), pp. 25–48.

Kantha, L H., P. E. Pontius, and V. Anantharaj, "Tides in Marginal and Semi-Enclosed and Coastal Seas, Part I: Sea Surface Height," Mississippi State University, http://www.cast.msstate.edu/Tides2D, 1994.

Kantha, L. H., "Barotropic Tides in the Global Oceans from a Nonlinear Tidal Model Assimilating Altimetric Tides Part I: Model Description and Results," *J. Geophys. Res.* **100**(C12), 25,283–25,308 (1995).

Lee, S. and R. Beardsley, "Numerical Study of the M_2 Tide and Residual Currents in the Yellow Sea," Draft Report #2, Dec 1993.

Lee-Lueng, F., E. J. Christensen, C. A. Yamarone, M. Lefebvre, Y. Menard, M. Dorrer, and P. Escudier, "TOPEX/POSEIDON Mission Overview," *J. Geophys. Res.* **99**(C12), 24,369–24,381 (1994).

LeProvost, C., M. L. Genco, F. Lyard, P. Vincent, and P. Canceil, "Spectroscopy of the World Ocean Tides from a Finite Element Hydrodynamic Model," *J. Geophys. Res.* **99**(C12), 24,777–24,798 (1994).

Luettich, R. A., J. J. Westerink, and N. W. Scheffner, "ADCIRC: An Advanced Three-Dimensional Circulation Model for Shelves, Coasts, and Estuaries, Report 1: Theory and Methodology of ADCIRC-2DDI and ADCIRC-3DL," Tech. Rep. DRP-92-6, Department of the Army, Washington, D.C., 1992.

Lynch, D. R., and F. E. Werner, "Three-Dimensional Hydrodynamics on Finite Elements, Part II: Non-Linear Timestepping Model," *Int. J. Numer. Methods Fluids* **12**(6), 507–534 (1991).

O'Connor, W. P., "A User's Manual for the Princeton Numerical Ocean Model, Institute for Naval Oceanography SP-5," Naval Research Laboratory, Stennis Space Center, MS, Mar 1991.

Schwiderski, E. W., "On Charting Global Ocean Tides," *Rev. Geophys. Space Phys.* **18**, 243–268 (1980).

Smagorinsky, J., "General Circulation Experiment with the Primitive Equations, I. The Basic Experiment," *Mon. Weath. Rev.* **91**, 99–164 (1963).

Zhenxing, D., Y. Lianwu, and J. Ozer, "Numerical Simulation of Three-Dimensional Tidal Current in the Bohai Sea," *Acta Oceanologica Sinica*, **13**(2), 155–172 (1994).